Volume 14, Issue 4, 142443 (1-11)

Iranian Journal of Catalysis (IJC)

https://doi.org/10.57647/j.ijc.2024.1404.43

Fabrication of a new magnetic nanocatalyst and its application for the effectual construction of pyrimido[4,5-*b*]quinolines

Abdolkarim Zare[1,*], Marziyeh Barzegar[2], Ahmad Reza Moosavi-Zare[3,4,*]

[1]*Department of Chemistry, Faculty of Nano and Bio Science and Technology, Persian Gulf University, Bushehr, Iran.*
[2]*Department of Chemistry, Payame Noor University, Tehran, Iran.*
[3]*Chemistry Department, College of Sciences, Shiraz University, Shiraz, Iran.*
[4]*Department of Chemical Engineering, Hamedan University of Technology, Hamedan, Iran.*

[*]**Corresponding authors:** a.zare@pgu.ac.ir, a.moosavizare@saadi.shirazu.ac.ir

Original Research

Received:
27 May 2024
Revised:
24 September 2024
Accepted:
01 November 2024
Published online:
16 November 2024

Abstract:

A new magnetic nanocatalyst, namely $[Fe_3O_4@SiO_2@RNMe_2\text{-}SO_3H][CF_3CO_2]$ (FSRNSC), was fabricated, and characterized using FT-IR, EDS (energy-dispersive X-ray spectroscopy), elemental mapping, FE-SEM (field-emission scanning electron microscopy), XRD (X-ray diffraction), VSM (vibrating-sample magnetometry), TG (thermogravimetric) and DTG (differential thermogravimetric) analyses. It was utilized as a highly effectual and magnetically recoverable catalyst for the construction of pyrimido[4,5-*b*]quinolines (12 examples) in high yields (15 – 50 min) and short times (88 – 96%). The synthesis was performed through the one-pot, three-component reaction of aryl aldehydes, dimedone, and 6-amino-1,3-dimethyluracil in the absence of solvent.

Keywords: Magnetic nanocatalyst; $[Fe_3O_4@SiO_2@RNMe_2\text{-}SO_3H][CF_3CO_2]$; 6-Amino-1,3-dimethyluracil; Pyrimido[4,5-*b*]quinoline

1. Introduction

Magnetic nanomaterials are of great prominence, and abundant uses in various fields have been reported for them [1–28]. For instance, they have been used in wastewater treatment [1], supercapacitors [2], and biosensors [3]; the nanomaterials have also been utilized for microplastic separation and degradation [4], biomedical purposes [5], and catalyzing organic reactions [6–28]. Nano-Fe_3O_4 has unique properties to use as a good core for the production of functionalized magnetic nanomaterials; these properties consist of suitable stability (thermic and chemical), non-toxicity, superparamagnetic feature, facile isolation and recycling, ability to graft with diverse functional groups, and straightforward synthesis procedures [10–28].

Multi-component reactions (MCRs) and solvent-free conditions are practical and highly efficacious approaches in synthetic organic chemistry, and their privileges have been reported in scientific sources. Application of these techniques in organic synthesis leads to higher yields of products, shorter reaction times, saving energy and cost, decreased waste production, reduced use of harmful organic solvents, and good matching with green chemistry protocols [29–38].

Pyrimido-quinoline, pyrimidine, quinoline, and uracil moieties are found in the scaffolds of numerous bioactive and medicinal substances. As examples, uracil and pyrimidine-containing compounds are utilized as gonadotropin-releasing hormone receptor antagonists [39], carbonic anhydrase inhibitors [40], and anti-inflammatory

[41] agents. Pyrimido-quinoline unit is found in compounds that have antimalarial [42], antitumor [43], antiallergic [44], antifungal [45], and analgesic [46] properties. Quinoline-bearing heterocycles can be applied as P-selectin antagonistic [47], anti-inflammatory [48], anticancer [18], and cyclooxygenase-2 inhibitory [49] agents. Pyrimido[4,5-*b*]quinolines have uracil, pyrimidine, pyramid-quinoline, and quinoline moieties and can be synthesized via the one-pot MCR of aryl aldehydes, dimedone, and 6-amino-1,3-dimethyluracil using a catalyst [50–61]. Considering the high prominence of pyrimido[4,5-*b*]quinolines, introducing new efficient catalysts for their synthesis is of significant interest.

In this project, we report the use of magnetic nanocatalyst, MCR and solvent-free conditions for the fabrication of pyrimido[4,5-*b*]quinolines. We have constructed, fully characterized, and applied [Fe_3O_4@SiO_2@$RNMe_2$-SO_3H][CF_3CO_2] (FSRNSC), as a novel magnetic nanocatalyst, to prepare of the mentioned compounds.

2. Experimental

2.1 Materials and apparatuses

Details of this section have been described in supplementary material.

2.2 Fabrication of FSRNSC (Scheme 1)

Nano-Fe_3O_4 was fabricated thru the published method [62, 63]. Thereafter, a mixture of nano-Fe_3O_4 (1.16 g), $Si(OEt)_4$ (3.5 mL), EtOH (93 mL), H_2O (23 mL), and NH_3 solution (3.5 mL) was stirred and refluxed for 12 h to generate **I** [62–64]. (3-chloropropyl)trimethoxysilane (0.92 g, 5 mmol) was added to compound **I** in toluene (40 mL) and stirred under reflux conditions for 12 h to construct **II** [62–64]. In continue, N^1,N^1,N^2,N^2-tetramethylethane-1,2-diamine (5 mmol, 0.75 mL) was added to **II** in toluene (30 mL), and stirred in reflux conditions for 12 h, wherein substance **III** was manufactured [56]. **III** was slowly added to a stirring solution of $ClSO_3H$ (5 mmol, 0.34 mL) in dry CH_2Cl_2 (25 mL) at 10 °C, and stirred for 5 h at ambient temperature, in which **IV** was acquired. Eventually, a solution of CF_3CO_2H (0.57 mL) in dry CH_2Cl_2 (15 mL) was gently poured to **IV** at ambient temperature and stirred for 10 h at this temperature and 2 h in reflux conditions to fabricate FSRNSC.

Note: Before each stage, ultrasound irradiation was applied for dispersion of the reaction mixture. The acquired substance in each stage was detached by a magnet, washed by the utilized solvent in that stage, and dried.

2.3 The construction of pyrimido[4,5-*b*]quinolines

A mixture of aldehyde (1 mmol), 6-amino-1,3-dimethyluracil (1 mmol, 0.155 g), dimedone (1 mmol, 0.140 g), and FSRNSC (0.048 g) in a test tube mounted in an oil bath was stirred strongly with a glass rod at 120 °C (the stirring was done by hand). After consumption of the reactants (affirmed by TLC) and cooling the mixture to ambient temperature, EtOAc (40 mL) was added, stirred, and refluxed for 2 min, and FSRNSC was detached by a magnet, washed by EtOAc, and dried. The EtOAc portion that remained after the magnetic separation was distilled to produce a solid, which was recrystallized from EtOH (95%) to construct the pure compound. The known pyramid-quinolines were recognized by matching their melting points with the literature data, as noted in Table 4; representative spectra are provided below.

Pyrimido[4,5-b]quinoline ***4c***

^{1}H NMR (500 MHz, DMSO-d_6, ppm): δ 0.88 (s, 3H, CH_3–C), 1.03 (s, 3H, CH_3–C), 1.97 (d, J = 16.1 Hz, 1H, one H of CH_2–C=C), 2.19 (d, J = 16.0 Hz, 1H, one H of CH_2–C=C), 2.55 – 2.59 (AB system, 2H, CH_2–C=O), 3.04 (s, 3H, CH_3–N), 3.45 (s, 3H, CH_3–N), 5.16 (s, 1H, CH–Ar), 7.08 (t, J = 6.9 Hz, 1H, H_{Ar}), 7.16 (t, J = 6.9 Hz, 1H, H_{Ar}), 7.20 (d, J = 7.6 Hz, 1H, H_{Ar}), 7.33 (d, J = 7.2 Hz, 1H, H_{Ar}), 8.99 (s, 1H, NH); ^{13}C NMR (125 MHz, DMSO-d_6, ppm): δ 26.3, 27.5, 29.1, 30.2, 30.7, 31.9, 33.7, 50.1, 89.5, 110.8, 126.3, 127.3, 129.1, 132.0, 132.6, 143.4, 144.1, 149.8, 150.5, 160.5, 194.3.

Pyrimido[4,5-b]quinoline ***4e***

^{1}H NMR (500 MHz, DMSO-d_6, ppm): δ 0.89 (s, 3H, CH_3–C), 1.05 (s, 3H, CH_3–C), 2.06 (d, J = 16.0 Hz, one H

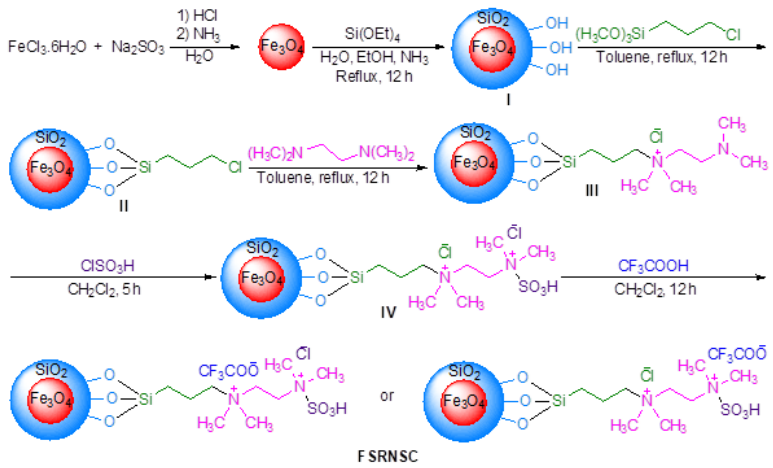

Scheme 1. The fabrication of FSRNSC.

of CH_2–C=C), 2.23 (d, J = 15.9 Hz, one H of CH_2–C=C), 2.56 – 2.63 (AB system, 2H, CH_2–C=O), 3.10 (s, 3H, CH_3–N), 3.46 (s, 3H, CH_3–N), 4.87 (s, 1H, CH–Ar), 7.09 – 7.40 (AB system, 4H, H_{Ar}), 9.04 (s, 1H, NH).

Pyrimido[4,5-b]quinoline ***4i***

IR (KBr disk, cm^{-1}): ν_{max} 1242, 1288, 1382, 1501, 1609, 1663, 1698, 2961, 3086, 3202; ^{1}H NMR (500 MHz, DMSO-d_6, ppm): δ 0.89 (s, 3H, CH_3–C), 1.03 (s, 3H, CH_3–C), 2.03 (d, J = 15.7 Hz, 1H, one H of CH_2–C=C), 2.20 (d, J = 15.4 Hz, 1H, one H of CH_2–C=C), 2.50 – 2.60 (AB system, 2H, CH_2–C=O), 3.08 (s, 3H, CH_3–N), 3.44 (s, 3H, CH_3–N), 4.81 (s, 1H, CH–Ar), 5.00 (s, 2H, CH_2–O), 6.81 (d, J = 5.3 Hz, 2H, H_{Ar}), 7.11 (d, J = 5.6 Hz, 2H, H_{Ar}), 7.30 – 7.40 (m, 5H, H_{Ar}), 8.97 (s, 1H, NH); ^{13}C NMR (125 MHz, DMSO-d_6, ppm): δ 26.5, 27.6, 29.1, 30.1, 32.1, 32.9, 50.1, 69.1, 90.3, 111.9, 113.9, 127.6, 127.7, 128.4, 128.6, 137.3, 138.9, 143.6, 149.2, 150.5, 156.6, 160.7, 194.5; Mass (EI, 70 eV): m/z 471 (M^+).

3. Results and discussion

3.1 Characterization of FSRNSC

Coating SiO_2 on the nano-Fe_3O_4 core and bonding the organic constituent to the SiO_2 surface, and consequently, successful fabrication of [Fe_3O_4@SiO_2@$RNMe_2$-SO_3H][CF_3CO_2] were affirmed by FT-IR spectroscopy (Figure 1). The obtained data of FT-IR analysis and their interpretation are given in Table 1; in the spectra, all expected bonds in the structure of FSRNSC were seen; the scientific data verified the interpretations [56, 65].

Existing silicon (relevant to SiO_2 and Si-R), oxygen (pertained to Fe_3O_4, SiO_2, SO_3H and $CF_3CO_2^-$), iron (related to Fe_3O_4), carbon (appertained to the organic chain and $CF_3CO_2^-$), nitrogen (belong to NMe_2), sulfur (related to SO_3H), chlorine (pertinent to Cl^-) and fluorine (relevant to $CF_3CO_2^-$) in the structure of [Fe_3O_4@SiO_2@$RNMe_2^-SO_3H$][CF_3CO_2] was affirmed by EDS and elemental mapping analyses (Figures 2 and 3). Moreover, the pictures attained from the elemental mapping analysis (Figure 3) verified a good distribution of Si, O, Fe, C, N, S, Cl, and F on the surface of FSRNSC.

Size and morphology of the particles were characterized by FE-SEM analysis (Figure 4); as the gained micrograph demonstrates, the particles sizes are less than 100 nm (i.e. they can be defined as nanoparticles), and the particles have different crystalline shapes.

In the attained diagram from the XRD analysis of [Fe_3O_4@SiO_2@$RNMe_2$-SO_3H][CF_3CO_2] (Figure 5), some sharp peaks (at $2\theta \approx$ 25.3, 30.4, 35.9, 43.5, 54.0, 57.5, 62.9 and 74.8°) and a broad peak (at $2\theta \approx 10.6 - 33.0°$) appeared. The sharp peaks at $2\theta \approx$ 30.4, 35.9, 43.5, 54.0, 57.5, and 62.9° affirmed existing a cubic spinel structure of Fe_3O_4 in FSRNSC, and the broad peak ascribed to SiO_2 (amorphous structure). The FWHM (full width at half maximum), interplanar distance (d-spacing), relative intensity pertained to each peak, and the computed particle sizes of FSRNSC are given in Table 2. The particle sizes (D), which were computed by the Debye-Scherrer equation $D = K\lambda/(\beta cos\nu)$, were in the range of 8.47 – 24.26 nm.

To study the magnetic property of FSRNSC, VSM analy-

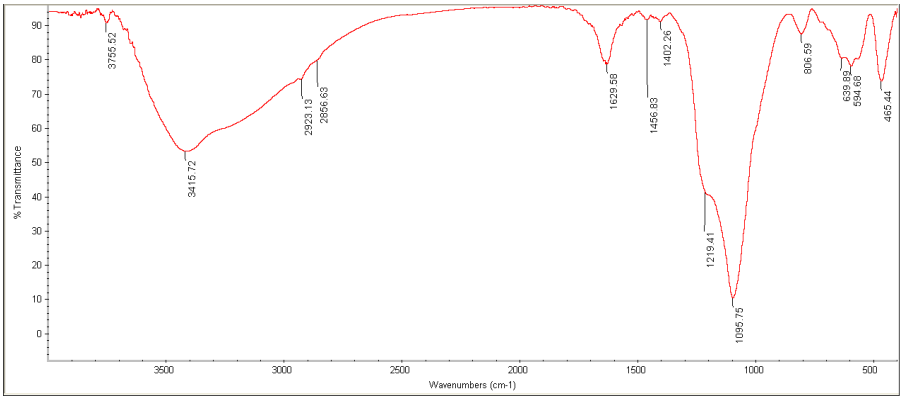

Figure 1. The FT-IR spectrum of FSRNSC.

Table 1. The FT-IR data of FSRNSC and their interpretation.

Peak (cm^{-1})	Relevant bond	Vibration type
465	Si–O	Rocking
595	Fe–O	-
640	S–O	Stretching
807	Si–O–Si	Symmetric stretching
1096	Si–O–Si	Asymmetric stretching
1457	C–H	Bending
2923	C–H	Stretching
2200-3720	OH groups of SO_3H	Stretching

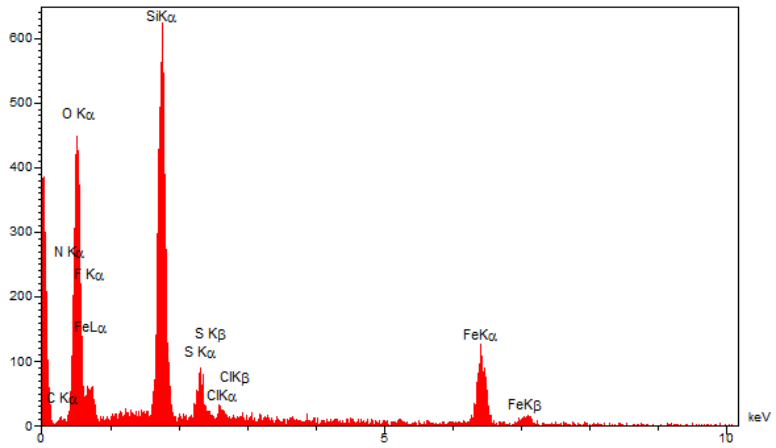

Figure 2. The EDS spectrum of FSRNSC.

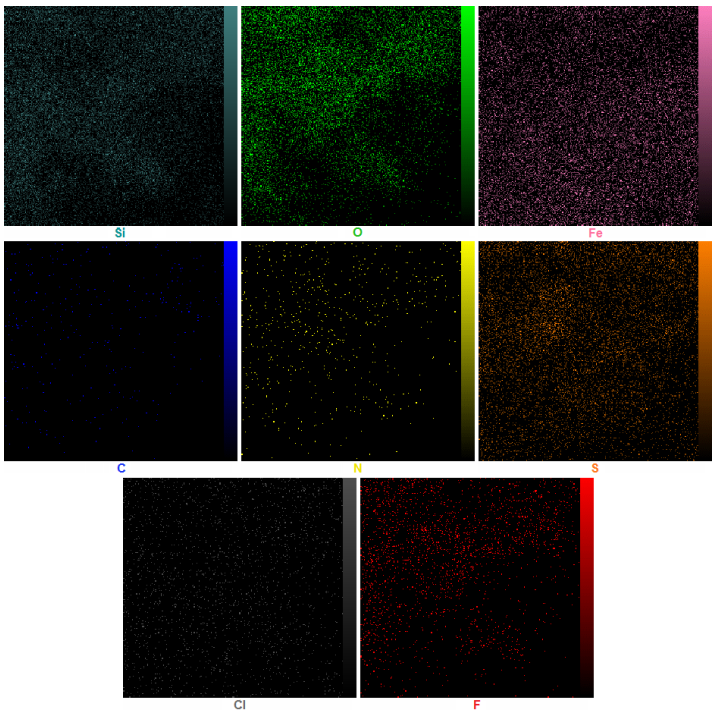

Figure 3. The elemental mapping pictures of $[Fe_3O_4@SiO_2@RNMe_2\text{-}SO_3H][CF_3CO_2]$.

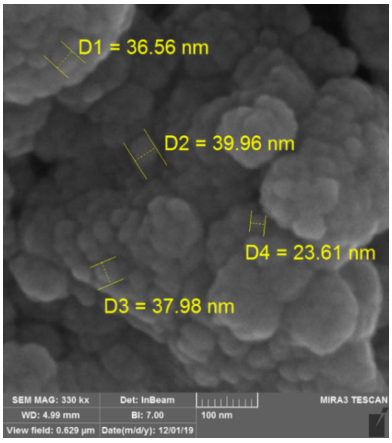

Figure 4. The FE-SEM micrograph of FSRNSC.

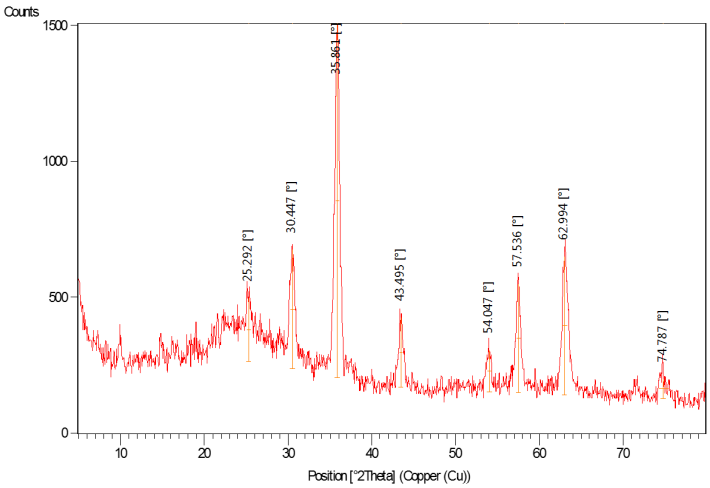

Figure 5. The XRD pattern of FSRNSC.

sis was utilized (Figure 6). Saturation magnetization (Ms) of $[Fe_3O_4@SiO_2@RNMe_2\text{-}SO_3H][CF_3CO_2]$ was ~20.7 emu/g. It should be mentioned that the Ms of the used nano-Fe_3O_4 for the fabrication of the nanocatalyst was ~56.7 emu/g [21]. The decrement of Ms in the nanocatalyst compared with nano-Fe_3O_4 is because of coating silica on the core and bonding $RNMe_2\text{-}SO_3H$ and $CF_3CO_2^-$ with the surface of $Fe_3O_4@SiO_2$.

The thermal consistency of the nanocatalyst was investigated using TG and DTG analyses (Figure 7); weight decrement of FSRNSC occurred in three stages. The first stage (below ~160 °C with T_{max} at 128 °C in the DTG diagram) seems to be because of evaporating the absorbed solvents on the surface of FSRNSC. The second stage (~160 – 380°C with T_{max} at 312 °C in the DTG diagram) can be ascribed to decomposing the $RNMe_2\text{-}SO_3H$ and $CF_3CO_2^-$ constituents. The third stage (~380 – 600°C with T_{max} at 538 °C in the DTG diagram) can be related to condensing the silanol groups. The literature data verified these explanations [33, 56].

Table 2. The XRD data of FSRNSC.

2θ (°)	FWHM (°)	d-spacing (nm)	Rel. int. (%)	Particle size (nm)
25.2920	0.5904	0.3521	17.66	13.47
30.4474	0.5904	0.2936	33.60	13.96
35.8610	0.3444	0.2504	100.00	24.26
43.4950	0.3936	0.2081	19.57	21.75
54.0470	0.5904	0.1697	11.61	15.12
57.5360	0.4920	0.1602	30.56	18.43
62.9942	0.6888	0.1476	39.05	13.54
74.7870	1.1808	0.1269	5.60	8.47

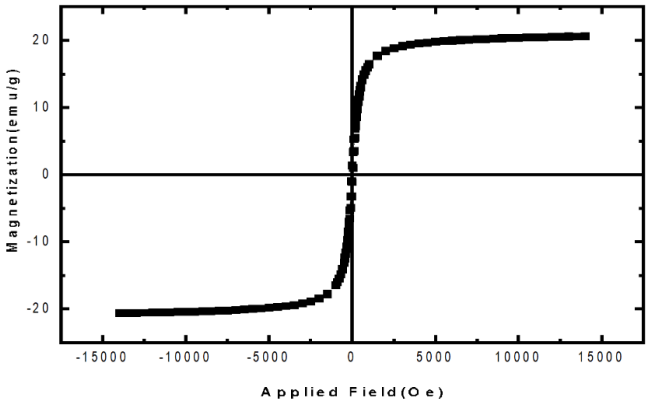

Figure 6. The VSM diagram of $[Fe_3O_4@SiO_2@RNMe_2\text{-}SO_3H][CF_3CO_2]$.

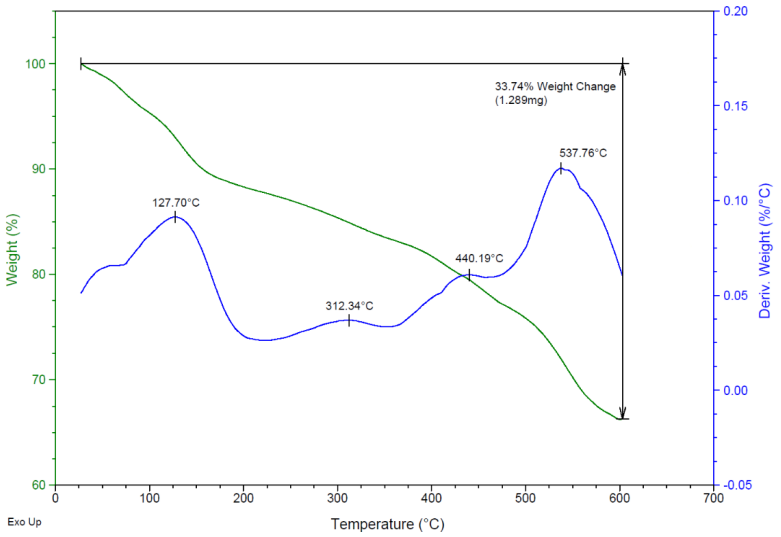

Figure 7. The TG and DTG diagrams of FSRNSC.

3.2 Catalytic performance of FSRNSC for the construction of pyrimido[4,5-*b*]quinoline

After full characterization of the magnetic nanocatalyst, we chose the one-pot MCR of 6-amino-1,3-dimethyluracil (1 mmol), 4-chlorobenzaldehyde (1 mmol), and dimedone (1 mmol) as a model (Scheme 2), and explored influence of different quantities of FSRNSC in a temperature range of 100 – 125°C on the reaction (solvent-free technique was used); the gained data are summed up in Table 3. Catalyst-free conditions afforded low yields of pyrimido[4,5-*b*]quinoline **4e** (entry 1). The optimal catalyst amount and temperature were found to be 0.048 g and 120 °C, respectively (entry 3). When the catalyst quantity was increased up to 0.055 g, or the reaction temperature was enhanced up to 125 °C, the results did not improve (entries 4 and 6).

After studying the catalytic activity of FSRNSC on the model reaction and observing its high efficacy under the optimum conditions, we investigated the reaction scope. Thus, diverse aryl aldehydes were reacted with dimedone and 6-amino-1,3-dimethyluracil; the reaction times, yields, and melting points are displayed in Table 4. We surveyed aryl aldehydes bearing electron-donating and electron-withdrawing substitutions on *ortho*, *meta*, and *para* positions and also disubstituted aldehydes. The reaction outcomes did not seem to be very dependent on the nature or number of substituent groups, and all aldehydes afforded excellent yields of the relevant products in short reaction times, suggesting that FSRNSC is a general and highly performance catalyst for this reaction.

Table 5 gives a comparison of FSRNSC with some previous catalysts for the construction of pyrimido[4,5-*b*]quinolines

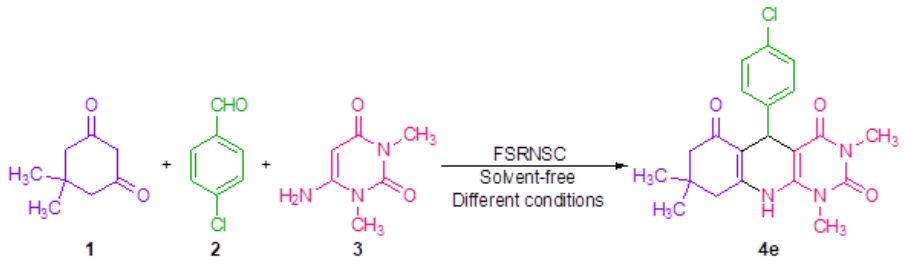

Scheme 2. The model reaction for optimizing the catalyst quantity and temperature.

Table 3. Optimization of the catalyst quantity and the reaction temperature (Scheme 2).

Entry	Quantity of FSRNSC (g)	Temp. (°C)	Time (min)	Yield (%)
1	-	120	60	27
2	0.040	120	25	89
3	0.048	120	15	95
4	0.055	120	15	95
5	0.048	110	30	86
6	0.048	125	15	95

Table 4. The fabrication of pyrimido[4,5-*b*]quinoline derivatives using FSRNSC.

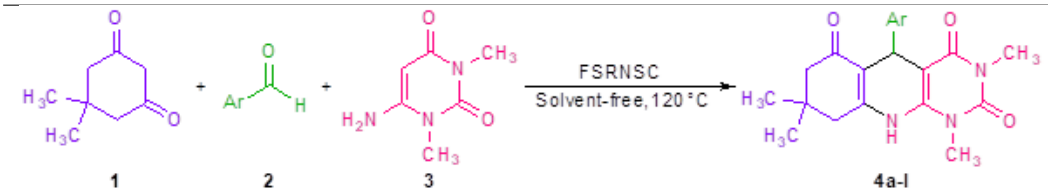

1 2 3 4a-l

Compd. No.	Ar	Time (min)	Yield[a] (%)	M.p. (°C) [Lit.]
4a	C_6H_5	15	96	273 – 275 (271 – 273) [51]
4b	3-BrC_6H_4	15	96	278 – 280 (280 – 283) [52]
4c	2-ClC_6H_4	15	88	321 – 323 (324 – 326) [56]
4d	2,4-$Cl_2C_6H_3$	15	95	317 – 319 (319 – 321) [56]
4e	4-ClC_6H_4	15	95	294 – 296 (290 – 292) [55]
4f	4-$CH_3C_6H_4$	15	95	308 – 310 (305 – 308) [61]
4g	4-HOC_6H_4	20	91	307 – 309 (310 – 312) [56]
4h	4-$CH_3OC_6H_4$	15	96	299 – 301 (301 – 303) [51]
4i	4-($C_6H_5CH_2O$)C_6H_4	15	93	289 – 291 (295 – 299) [50]
4j	2,5-$(CH_3O)_2CV6H_3$	20	94	207 – 210 (208 – 210) [51]
4k	3,4-$(CH_3O)_2C_6H_3$	15	95	295 – 297 (298 – 300) [56]
4l	4-[$(CH_3)_2N$]C_6H_4	50	93	256 – 258 (253 – 255) [61]

[a]Isolated yield.

4a, **4e** and **4h**. Our catalyst afforded the products in higher yields in comparison with most of the other catalysts; the reaction times of FSRNSC were shorter than those of the catalysts reported in entries 2 – 8 and 10. Moreover, in the present method, we used solvent-free conditions, which are in accordance with green chemistry protocols. But, the reaction temperature of our method is higher than most of the catalysts reported in Table 4. It is worth noting that our new protocol has improved the range of yields when compared with our published methods [50, 56, 61]. In general, we feel that this method is among the best for the fabrication of pyrimido[4,5-*b*]quinolines.

The recoverability of FSRNSC was surveyed for the fabrication of product **4e**; it was recovered pursuant to the method given in the Experimental section. When the fresh [Fe_3O_4@SiO_2@$RNMe_2$-SO_3H][CF_3CO_2] was utilized, the reaction yield and time were 95% and 15 min, correspondingly. In the first recovery of FSRNSC, the reaction yield and time were 20 min and 93%, respectively. In the second recovery, the yield was diminished to 82%, and the reaction time was enhanced by up to 35 min. Thus, FSRNSC was recoverable and reusable for one time with an insignificant decrement of catalytic performance, but, in the second recycling, its catalytic performance was decreased.

Table 5. Comparing outcomes and the reaction conditions of FSRNSC with those of the reported catalysts for the construction of pyrimido[4,5-*b*] quinolines **4a**, **4e**, and **4h**.

Entry	Catalyst	Conditions	Time (min) of product **4a/4e/4h**	Yield (%) of product **4a/4e/4h**	Ref.
1	FSRNSC	Solvent-free, 120 °C	15/15/15	96/95/96	–
2	[TSSECM][a]	Solvent-free, 125 °C	40/40/30	93/92/95	[51]
3	Fe_3O_4NPs-cell[b]	H_2O, reflux	120/120/120	89/91/87	[52]
4	$CoFe_2O_4$@SiO_2@$Si(CH_2)_3NHCOOCH_2COOH$	EtOH, reflux	–[c]/45/75	–[c]/97/93	[53]
5	[H_2-DABCO][HSO_4]$_2$	H_2O/EtOH, 75 °C	65/70/–[c]	90/93/–[c]	[54]
6	$InCl_3$	H_2O, reflux	–[c]/60/60	–[c]/91/89	[55]
7	Choline chloride/oxalic acid	80 °C	45 – 60[d]	92 – 98[d]	[57]
8	Fe_3O_4@Cellulose-SO_3H	H_2O, 80 °C	20/20/30	95/90/87	[58]
9	[dsim]HSO_4[e]	EtOH, 70 °C	–[c]/15/25	–[c]/91/85	[59]
10	TrCl	$CHCl_3$, reflux	130/130/130	79/88/75	[60]

[a]*N,N,N′,N′*-Tetramethyl-*N*-(silica-*n*-propyl)-*N′*-sulfonic acid-ethylenediaminium chloride/mesylate.

[b]Fe_3O_4 nanoparticles supported on cellulose.

[c]In the work, this compound has not been prepared.

[d]In the work, products **4a**, **4e** and **4h** have not been synthesized; thus, we have reported ranges of times and yields.

[e]1,3-Disulfonic acid imidazolium hydrogen sulfate.

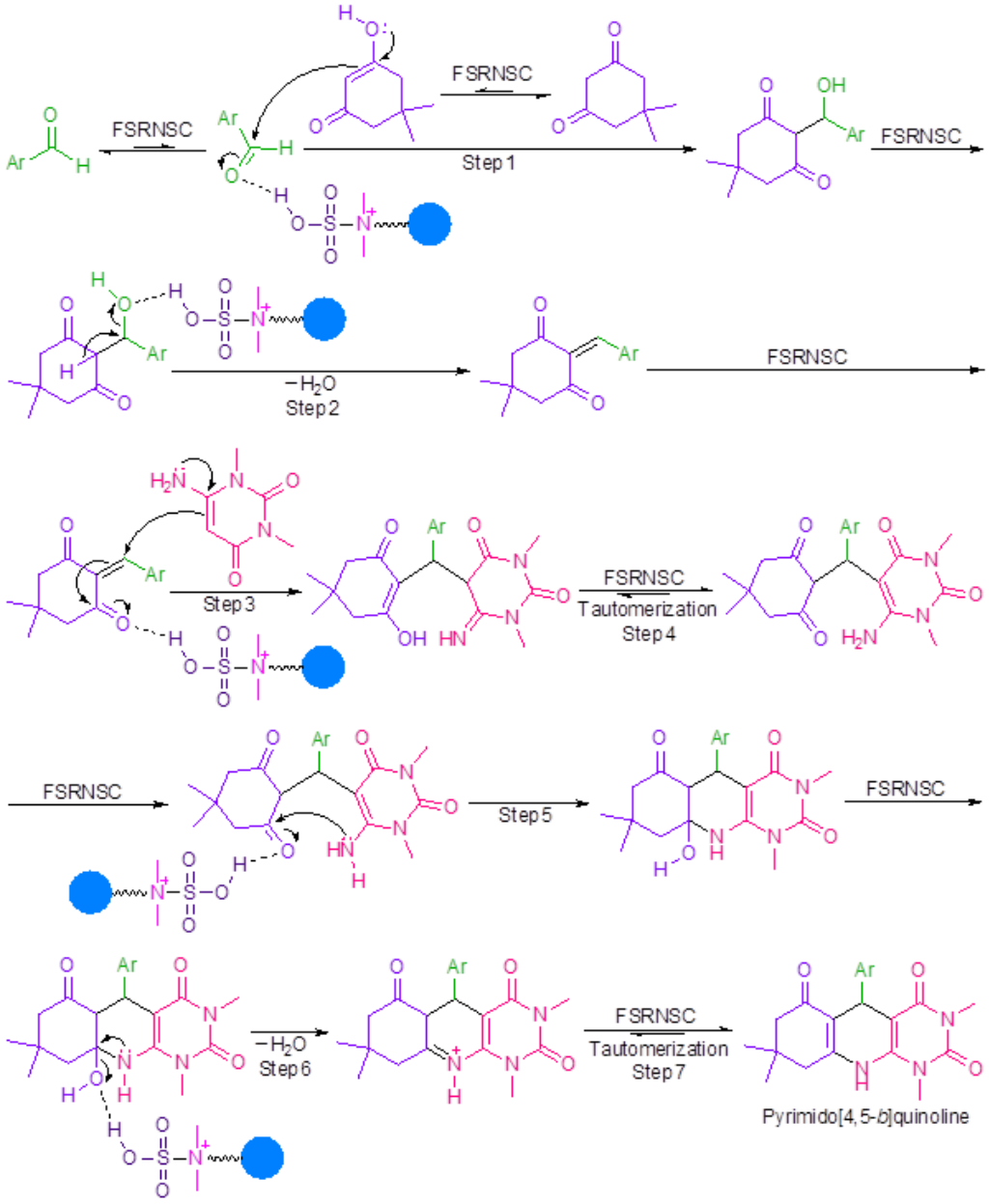

Scheme 3. The mechanism.

The catalyst roles are clearly illustrated in Scheme 3. The electrophiles are activated by the acidic hydrogen of FSRNSC, and then, nucleophilic addition reactions are performed (steps 1, 3 and 5). Removal of H_2O is also facilitated by the acidic hydrogen (steps 2 and 6). Moreover, FSRNSC can accelerate tautomerization reactions (steps 1, 4 and 7). The literature information support the suggested mechanism [54, 56].

4. Conclusion

In summary, a novel acidic magnetic nanocatalyst, namely $[Fe_3O_4@SiO_2@RNMe_2\text{-}SO_3H][CF_3CO_2]$, has been introduced. It may catalyze organic reactions that need acidic catalysts to carry out; in this work, the construction of pyrimido[4,5-*b*]quinoline derivatives has been catalyzed by $[Fe_3O_4@SiO_2@RNMe_2\text{-}SO_3H][CF_3CO_2]$. The benefits of this protocol consist of high performance, short reaction times, excellent yields, low catalyst loading, usage of solvent-free conditions, and good consistency with green chemistry principles.

Acknowledgments

Support of this project by Payame Noor University is gratefully acknowledged by the authors.

Authors Contributions
Authors were equally contributed in acquisition and analysing the data as well as preparing the paper.

Availability of Data and Materials
Data is available on request from the corresponding author, upon reasonable request.

Conflict of Interests
The authors declare that they have no known competing financial interests or personal relationships that could have appeared to influence the work reported in this paper.

References

[1] S. Ramu, I. Kainthla, L. Chandrappa, J.M. Shivanna, B. Kumaran, and R.G. Balakrishna. *Environ. Sci. Pollut. Res.*, **31**(2024):167–190. DOI: https://doi.org/10.1007/s11356-023-31162-8.

[2] M. Haghshenas, M. Mazloum-Ardakani, F. Tamaddon, and A. Nasiri. *Int. J. Hydrog. Energy*, **46**(2021):3984–3995. DOI: https://doi.org/10.1016/j.ijhydene.2020.10.253.

[3] F.M.A. Altalbawy, E. Ali, Y.F. Mustafa, A.A. Ibrahim, S. Mansouri, D.O. Bokov, A. Alawadi, A. Saxena, A. Alsaalamy, and S.K. Oudah. *J. Taiwan Inst. Chem. Eng.*, **157**(2024):105410. DOI: https://doi.org/10.1016/j.jtice.2024.105410.

[4] Y. Cao, C. Sathish, X. Guan, S. Wang, T. Palanisami, A. Vinu, and J. Yi. *J. Hazard. Mater.*, **461**(2024):132537. DOI: https://doi.org/10.1016/j.jhazmat.2023.132537.

[5] T.I. Shabatina, O.I. Vernaya, V.P. Shabatin, and M.Y. Melnikov. *Magnetochemistry*, **6**(2020):30. DOI: https://doi.org/10.3390/magnetochemistry6030030.

[6] M.A. Khajeh Shahkoei, A. Yahyazadeh, and A. Dehno Khalaji. *Inorg. Chem. Res.*, **7**(2023):34–41. DOI: https://doi.org/10.22036/j10.22036.2024.423255.1154.

[7] H. Atharifar, A. Keivanloo, B. Maleki, M. Baghayeri, and H. Alinezhad. *Res. Chem. Intermed.*, **50**(2024): 281–296. DOI: https://doi.org/10.1007/s11164-023-05152-x.

[8] R. Jahanshahi, A. Khazaee, S. Sobhani, and J.M. Sansano. *New J. Chem.*, **44**(2020):11513–11526. DOI: https://doi.org/10.1039/D0NJ01599G.

[9] M. Foroughi Kaldareh, M. Mokhtary, and M. Nikpassand. *Appl. Organomet. Chem.*, **34**(2020):e54692020. DOI: https://doi.org/10.1002/aoc.5469.

[10] M. Hosseinzehi, M.H. Ehrampoush, F. Tamaddon, M. Mokhtari, and A. Dalvand. *Int. J. Environ. Anal. Chem.*, **103**(2023):4339–4359. DOI: https://doi.org/10.1080/03067319.2021.1928096.

[11] F. Rezaei, H. Alinezhad, and B. Maleki. *Sci. Rep.*, **13**(2023):20562. DOI: https://doi.org/10.1038/s41598-023-47794-2.

[12] N. Karami, A. Mohammadpour, M.R. Samaei, A.M. Amani, M. Dehghani, R.S. Varma, and J.N. Sahu. *Int. J. Biol. Macromol.*, **254 (Part 1)**(2024):127663. DOI: https://doi.org/10.1016/j.ijbiomac.2023.127663.

[13] K. Alizadeh, E. Khaledyan, and Y. Mansourpanah. *J. Appl. Organomet. Chem.*, **2**(2022):198–208. DOI: https://doi.org/10.22034/jaoc.2022.155004.

[14] F. Hakimi, M. Taghvaee, and E. Golrasan. *Adv. J. Chem. A*, **6**(2023):188–197, . DOI: https://doi.org/10.22034/AJCA.2023.393949.1364.

[15] N. Azgomi and M. Mokhtary. *J. Mol. Catal. A: Chem.*, **398**(2015):58–64. DOI: https://doi.org/10.1016/j.molcata.2014.11.018.

[16] A. Barzkar and A. Salimi Beni. *Sci. Rep.*, **13**(2023): 10336. DOI: https://doi.org/10.1038/s41598-023-36352-5.

[17] F.H. Mohammed, A.M. Aljeboree, A.N. Abd, A.F. Alkaimb, Y.S. Karim, S.A. Hamoodd, A.B. Mahdie, M.A. Jawadf, and S. Ahjelg. *Iran. J. Catal.*, **12**(2022):237–259. DOI: https://doi.org/10.30495/ijc.2022.1957195.1929.

[18] E. Jazinizadeh, A. Zare, S.S. Sajadikhah, M. Barzegar, and A. Kohzadian. *Res. Chem. Intermed.*, **48**(2022): 2059–2075. DOI: https://doi.org/10.1007/s11164-022-04854-y.

[19] N. Salarinejad, M. Dabiri, and S. Kazemi Movahed. *J. Taiwan Inst. Chem. Eng.*, **159**(2024):105496. DOI: https://doi.org/10.1016/j.jtice.2024.105496.

[20] M. Mokhtary. *J. Iran. Chem. Soc.*, **13**(2016):1827–1845. DOI: https://doi.org/10.1007/s13738-016-0900-4.

[21] M. Barzegar, A. Zare, A. Ghobadpoor, and M. Dianat. *Iran. J. Catal.*, **12**(2022):13–24. DOI: https://doi.org/10.30495/ijc.2022.688895.

[22] S.-M. Khatami, M. Khalaj, and M. Ghashang. *Iran. J. Catal.*, **13**(2023):475–485. DOI: https://doi.org/10.30495/IJC.2023.1993331.2039.

[23] A. Khazaei, A.R. Moosavi-Zare, F. Gholami, and V. Khakyzadeh. *Appl. Organomet. Chem.*, **30**(2016): 691–694. DOI: https://doi.org/10.1002/aoc.3491.

[24] S. Esmaili, A.R. Moosavi-Zare, and A. Khazaei. *RSC Adv.*, **12**(2022):5386–5394, . DOI: https://doi.org/10.1039/D2RA00213B.

[25] S. Esmaili, A. Khazaei, and A.R. Moosavi-Zare. *Polycycl. Aromat. Compd.*, **43**(2023):6615–6626, . DOI: https://doi.org/10.1080/10406638.2022.2123539.

[26] F. Hakimi, A. Sharifi-Zarchi, and E. Golrasan. *Chem. Methodol.*, **7**(2023):489–498, . DOI: https://doi.org/10.22034/chemm.2023.392041.1667.

[27] E. Mohamadzadehm and Z. Gordi. *Iran. J. Catal.*, **12**(2022):169–180. DOI: https://doi.org/10.30495/IJC.2022.689839.

[28] M.A. Nasseri, Z. Rezazadeh, M. Kazemnejadim, and A. Allahresani. *Dalton Trans.*, **49**(2020):10645–10660. DOI: https://doi.org/10.1039/D0DT01846E.

[29] S.M. Saied, M.Y. Saleh, and A.M. Hamdoon. *Iran. J. Catal.*, **12**(2022):189–205. DOI: https://doi.org/10.30495/IJC.2022.1955651.1924.

[30] A. Kohzadian, R. Fathollahi, M. Karami, E. Korani, and A. Zare. *Iran. J. Catal.*, **13**(2023):331–340. DOI: https://doi.org/10.30495/ijc.2023.1990117.2017.

[31] B. Maleki, M. Chahkandi, R. Tayebee, S. Kahrobaei, H. Alinezhad, and S. Hemmati. *Appl. Organomet. Chem.*, **33**(2019):e5118. DOI: https://doi.org/10.1002/aoc.5118.

[32] S. Mehrizi Marvast and E. Rostami. *Asian J. Green Chem.*, **8**(2024):261–277. DOI: https://doi.org/10.48309/AJGC.2024.430848.1469.

[33] A. Zare, A. Kohzadian, Z. Abshirini, S.S. Sajadikhah, J. Phipps, M. Benamarad, and M.H. Beyzavi. *New J. Chem.*, **43**(2019):2247–2257, . DOI: https://doi.org/10.1039/C8NJ04921A.

[34] A.R. Moosavi-Zare and H. Afshar-Hezarkhani. *Org. Prep. Proced. Int.*, **52**(2020):410–421. DOI: https://doi.org/10.1080/00304948.2020.1787058.

[35] S. Sargazi Karbasaki, G. Bagherzade, B. Maleki, and M. Ghani. *J. Taiwan Inst. Chem. Eng.*, **118**(2021):342–354. DOI: https://doi.org/10.1016/j.jtice.2020.12.025.

[36] F. Karimi, M. Torabi, M. Yarie, M.A. Zolfigol, and Y. Gu. *J. Iran. Chem. Soc.*, **20**(2023):2189–2202. DOI: https://doi.org/10.1007/s13738-023-02794-x.

[37] M. Barzegar and A. Zare. *Prog. Chem. Biochem. Res.*, **5**(2022):68–76. DOI: https://doi.org/10.22034/pcbr.2022.326660.1210.

[38] L. Amiri-Zirtol, T. Solymani Ahooie, E. Riazimontazer, M.A. Amrollahi, and B.F. Mirjalili. *Sci. Rep.*, **13**(2023):17966. DOI: https://doi.org/10.1038/s41598-023-44521-9.

[39] S.-M. Kim, M. Lee, S.Y. Lee, S.-M. Lee, E.J. Kim, J.S. Kim, J. Ann, J. Lee, and J. Lee. *Eur. J. Med. Chem.*, **145**(2018):413–424. DOI: https://doi.org/10.1016/j.ejmech.2017.12.095.

[40] E.A. Türkoğlu, M. Şentürk, C.T. Supuran, and D. Ekinci. *J. Enzyme Inhib. Med. Chem.*, **32**(2017):74–77. DOI: https://doi.org/10.1080/14756366.2016.1235043.

[41] P. Yadav and K. Shah. *Chem. Biol. Drug Des.*, **97**(2021):633–648. DOI: https://doi.org/10.1111/cbdd.13800.

[42] A.A. Joshi and C.L. Viswanathan. *Bioorg. Med. Chem. Lett.*, **16**(2006):2613–2617. DOI: https://doi.org/10.1016/j.bmcl.2006.02.038.

[43] H.I. Ali, K. Tomita, E. Akaho, M. Kunishima, Y. Kawashima, T. Yamagishi, H. Ikeya, and T. Nagamatsu. *Eur. J. Med. Chem.*, **43**(2008):1376–1389. DOI: https://doi.org/10.1016/j.ejmech.2007.10.011.

[44] T.H. Althuis, P.F. Moore, and H.J. Hess. *J. Med. Chem.*, **22**(1979):44–48. DOI: https://doi.org/10.1021/jm00187a011.

[45] S.M. Abdel-Gawad, M.S.A. El-Gaby, H.I. Heiba, H.M. Ali, and M.M. Ghorab. *J. Chin. Chem. Soc.*, **52**(2005):1227–1236. DOI: https://doi.org/10.1002/jccs.200500177.

[46] A.-R.B.A. El-Gazzar, M.M. El-Enany, and M.N. Mahmoud. *Bioorg. Med. Chem.*, **16**(2008):3261–3273. DOI: https://doi.org/10.1016/j.bmc.2007.12.012.

[47] N. Kaila, K. Janz, S. DeBernardo, P.W. Bedard, R.T. Camphausen, S. Tam, D.H.H. Tsao, J.C. Keith, C. Nickerson-Nutter, A. Shilling, R. Young-Sciame, and Q. Wang. *J. Med. Chem.*, **50**(2007):21–39. DOI: https://doi.org/10.1021/jm0602256.

[48] K.D. Upadhyay, N.M. Dodia, R.C. Khunt, R.S. Chaniara, and A.K. Shah. *ACS Med. Chem. Lett.*, **9**(2018):283–288. DOI: https://doi.org/10.1021/acsmedchemlett.7b00545.

[49] A. Zarghi, R. Ghodsi, E. Azizi, B. Daraie, M. Hedayati, and O.G. Dadrass. *Bioorg. Med. Chem.*, **17**(2009):5312–5317. DOI: https://doi.org/10.1016/j.bmc.2009.05.084.

[50] S. Esmaili, A.R. Moosavi-Zare, A. Khazaei, and Z. Najafi. *ACS Omega*, **7**(2022):45314–45324, . DOI: https://doi.org/10.1021/acsomega.2c05896.

[51] A. Zare, M. Dianat, and M.M. Eskandari. *New J. Chem.*, **44**(2020):4736–4743, . DOI: https://doi.org/10.1039/C9NJ06393E.

[52] L. Edjlali, R. Hosseinzdeh Khanamiri, and J. Abolhasani. *Monatsh. Chem.*, **146**(2015):1339–1342. DOI: https://doi.org/10.1007/s00706-014-1368-5.

[53] A. Gholami, M. Mokhtary, and M. Nikpassand. *Appl. Organomet. Chem.*, **34**(2020):e6007, . DOI: https://doi.org/10.1002/aoc.6007.

[54] F. Shirini, M. Safarpoor Nikoo Langarudi, N. Daneshvar, M. Mashhadinezhad, and N. Nabinia. *J. Mol. Liq.*, **243**(2017):302–312. DOI: https://doi.org/10.1016/j.molliq.2017.07.080.

[55] J.M. Khurana, A. Chaudhary, B. Nand, and A. Lumb. *Tetrahedron Lett.*, **53**(2012):3018–3022. DOI: https://doi.org/10.1016/j.tetlet.2012.04.001.

[56] A. Zare and M. Barzegar. *Res. Chem. Intermed.*, **46**(2020):3727–3740. DOI: https://doi.org/10.1007/s11164-020-04171-2.

[57] A. Gholami, M. Mokhtary, and M. Nikpassand. *Dyes Pigm.*, **180**(2020):108453, . DOI: https://doi.org/10.1016/j.dyepig.2020.108453.

[58] F. Osanlou, F. Nemati, and S. Sabaqian. *Res. Chem. Intermed.*, **43**(2017):2159–2174. DOI: https://doi.org/10.1007/s11164-016-2752-z.

[59] K. Mohammadi, F. Shirini, and A. Yahyazadeh. *RSC Adv.*, **5**(2015):23586–23590. DOI: https://doi.org/10.1039/C5RA02198G.

[60] A.R. Moosavi-Zare and R. Najafi. *Sci. Rep.*, **13**(2023):16501. DOI: https://doi.org/10.1038/s41598-023-43793-5.

[61] A. Zare, N. Lotfifar, and M. Dianat. *J. Mol. Struct.*, **1211**(2020):128030, . DOI: https://doi.org/10.1016/j.molstruc.2020.128030.

[62] M.A. Zolfigol, R. Ayazi-Nasrabadi, and S. Baghery. *Appl. Organomet. Chem.*, **30**(2016):500–509, . DOI: https://doi.org/10.1002/aoc.3461.

[63] S. Qu, H. Yang, D. Ren, S. Kan, G. Zou, D. Liand, and M. Li. *J. Colloid Interface Sci.*, **215**(1999):190–192. DOI: https://doi.org/10.1006/jcis.1999.6185.

[64] Y.H. Deng, C.C. Wang, J.H. Hu, W.L. Yang, and S.K. Fu. *Colloids Surf. A: Physicochem. Eng. Aspects*, **262**(2005):87–93. DOI: https://doi.org/10.1016/j.colsurfa.2005.04.009.

[65] M.A. Zolfigol, R. Ayazi-Nasrabadi, and S. Baghery. *Appl. Organomet. Chem.*, **30**(2016):273–281, . DOI: https://doi.org/10.1002/aoc.3428.